Catalysis Today 157 (2010) 436–439

Contents lists available at ScienceDirect

Catalysis Today

journal homepage: www.elsevier.com/locate/cattod

CO_2 reforming of methane over Ce-Zr-Ni-Me mixed catalysts

B. Koubaissy, A. Pietraszek, A.C. Roger, A. Kiennemann *

LMSPC, Laboratoire de Matériaux, Surfaces et Procédés pour la Catalyse, UMR 7515 du CNRS-ECPM-ULP, 25 Rue Becquerel, 67087 Strasbourg Cedex 2, France

ARTICLE INFO

Article history:
Available online 26 February 2010

Keywords:
Methane dry reforming
Nickel catalyst
Ce-Zr solid solution

ABSTRACT

Pseudo sol–gel method was applied to prepare monometallic as well as bimetallic catalysts, on the base of Ce-Zr mixed oxide, effective for dry reforming of methane. The monometallic catalysts with varying proportions of Ce and Zr and constant Ni loading (5 wt.%) were made to find the most effective system. On the basis of the results of the activity of the monometallic catalysts, three bimetallic catalysts were synthesised, where part of Ni was substituted by Co, Fe or Rh. The as prepared catalysts were characterized by powder X-ray diffraction (XRD), thermo-programmed reduction (TPR) and examined in CO_2 reforming of methane reaction. It was found that $Ce_2Zr_{1.51}Ni$ catalyst demonstrated the highest activity in CO_2 reforming of CH_4 among all the monometallic catalysts with CO_2 conversion ca. 80% at 750 °C. Ageing of the catalyst during 25 h time on stream conducted to the decrease of CO_2 conversion from 80% to 57% (750 °C). In the case of $Ce_2Zr_{1.51}NiRh$ catalyst CO_2 conversion increased up to 90% (750 °C). The ageing experiment demonstrated very high stability over 200 h with the conversion of 80%.

1. Introduction

One of the ways of chemical valorisation of natural gas is its transformation into synthesis gas (H_2 + CO). Nowadays, hydrogen is produced during the steam reforming of hydrocarbons. Another possibility is the partial oxidation of methane. Nevertheless, in recent years, the dry reforming of methane has become an interesting alternative for synthesis gas production. This endothermic process produces a H_2/CO ratio ≈1 which could be useful to adjust syngas ratio obtained from steam reforming process. The main drawback of this process is the catalyst deactivation due to the carbon deposition originated from methane decomposition and/or Boudard reaction and/or sintering of the metallic phase and support [1,2].

Nickel-based catalysts are commonly used in dry reforming of methane as they are effective in hydrogen production. Although noble metals such as Pt, Pd, Rh and Ru are reported to be more effective than nickel catalysts [3–5] they are not used in industrial applications due to their high costs. Despite the economical reason of using Ni catalysts, the main problem bounded with high deactivation rate still remains. To diminish the carbon formation due to enhancement of the metal/support interaction, the active phase incorporation into support structure of high oxygen mobility is proposed [6–8].

Catalytic activity and thermal stability of Ni-based catalysts could be improved by using mixed Ce-Zr oxide as a support. It is well known that CeO_2-ZrO_2 solid solution has good thermal stability and better oxygen storage capacity than CeO_2 alone [7,9,10]. This oxygen vacancy is also important for the dissociative adsorption of CO_2.

In this paper, the application of Ce-Zr catalysts, with Ni and/or Ni-Me (Me = Co, Fe, Rh) incorporated into the structure, in dry reforming of methane is examined. The physico-chemical characterization of the catalysts' structure as well as the influence of varying Ce and Zr contents and addition of second metal on the catalysts' activity and ageing is evaluated.

2. Experimental

2.1. Catalyst preparation

Various Ce-Zr-Ni-Me catalysts were prepared by pseudo sol–gel method based on thermal decomposition of metallic propionates [11,12]. The metal precursors used for synthesis were: cerium (III) acetate sesquihydrate, zirconium (IV) acetylacetonate, rhodium (II) acetate, nickel (II) acetate hydrate, cobalt (II) acetate hydrate and iron (II) acetate anhydrous. The salts were dissolved in excess of propionic acid. The solutions were mixed and heated under reflux. The solvent was evaporated to obtain gel which was then calcined in air at 750 °C during 4 h. The formulas of as prepared catalysts are summarized in Table 1.

* Corresponding author. Tel.: +33 0 368 85 27 66; fax: +33 0 3 68 85 27 68.
E-mail address: kiennemann@unistra.fr (A. Kiennemann).

0920-5861/$ – see front matter © 2010 Elsevier B.V. All rights reserved.
doi:10.1016/j.cattod.2010.01.050

Table 1
Textural properties of support, nickel and nickel-metal catalysts.

Catalysts	Abbreviation	Ni nominal content (wt.%)	Me nominal content (wt.%)	BET surface area (m^2/g)	Lattice parameter (Å)	Support particle size (nm)
Ce_2Zr_2	CeZr	–	–	19	5.27	6
$Ce_2Zr_{1.51}Ni_{0.49}$	$Ce_2Zr_{1.51}Ni$	5	–	18	5.29	7
$Ce_{2.96}Zr_{0.53}Ni_{0.51}$	$Ce_{2.96}Zr_{0.53}Ni$	5	–	32	5.36	9
$Ce_{0.6}Zr_{2.97}Ni_{0.43}$	$Ce_{0.6}Zr_{2.97}Ni$	5	–	15	5.17	7
$Ce_2Zr_{1.51}Ni_{0.49}Co_{0.29}$	$Ce_2Zr_{1.51}NiCo$	3	2	11	5.30	7
$Ce_2Zr_{1.51}Ni_{0.49}Fe_{0.20}$	$Ce_2Zr_{1.51}NiFe$	3	2	15	5.29	5
$Ce_2Zr_{1.51}Ni_{0.49}Rh_{0.03}$	$Ce_2Zr_{1.5}NiRh$	4.5	0.5	21	5.30	6

2.2. Physico-chemical characterization

2.2.1. BET

The Specific BET surface area was determined by N_2 adsorption–desorption measurements at −196 °C in a Tristar gas adsorption system.

2.2.2. XRD

The crystalline structure of mixed oxides was determined by powder X-ray diffraction using Brucker D8 Advanced apparatus with Cu Kα radiation.

2.2.3. TPR

The reducibility of the catalysts was studied by thermo-programmed reduction (TPR) using 0.05 g sample heated from room temperature to 900 °C with a slope 15 °C/min. under hydrogen/argon flow.

2.3. Catalytic activity

The catalytic activity measurements were performed in a fixed bed quartz reactor. Prior to CO_2/CH_4 reaction, 0.1 g of catalyst was reduced in 5% H_2-95%Ar at 750 °C for 4 h (0.0025 L/min). After the pre-treatment, a feed mixture consisting of CH_4/CO_2/Ar 10/10/80 was introduced into reactor. The total space velocity was equal to 30 L h^{-1} g^{-1}.The reforming tests were studied with an increase of temperature from 550 °C to 800 °C with the stabilization of 2 h at each temperature. Some steady-state experiments at 750 °C were also performed to study the second metal addition to Ce-Zr system.

3. Results and discussion

3.1. Catalysts characterization

It can be seen (Table 1) that the BET specific surface area seems not to be associated with Ni incorporation but with varying Ce and Zr contents. The highest value was observed for the catalyst enriched in Ce.

Fig. 1 shows the XRD diffractograms of the Ce_2Zr_2 support (a) and Ce-Zr-Ni catalysts (b–d) with different Ce and Zr contents after calcination in air at 750 °C for 4 h. It can be clearly seen that the patterns match well to the face-centered cubic structure of $Ce_{0.6}Zr_{0.4}O_2$ (JCPDS 38-1439) in the case of support (a), Zr-rich $Ce_{0.6}Zr_{2.97}Ni$ catalyst (b) and $Ce_2Zr_{1.51}Ni$ one (c) and to face-centered cubic structure of $Ce_{0.75}Zr_{0.25}O_2$ (JCPDS 28-271) for Ce-rich $Ce_{2.96}Zr_{0.53}Ni$ catalyst (d). Nevertheless the small, broad diffraction patterns at $2\theta = 37.3°$ and 43.3° indexed as NiO, with (0 0 1) and (2 0 0) planes can also be observed (see Fig. 1 zoom). This phenomenon might be explained by the small rejection of Ni from the host Ce-Zr structure. The intensity of NiO diffraction patterns differs and increases with the increase in Ce content due to the competition between larger Zr^{4+} (84 pm) and smaller Ni^{2+} (69 pm) cations in the Ce-Zr structure. The highest intensity of NiO diffraction patterns was observed for the catalysts enriched in Ce (Fig. 1(c and d)). The diffraction patterns position of the cubic fluorite varies with changing the fluorite stoichiometry according to Ce to Zr ratio. The structure modification is not associated with the introduction of Ni or other metals. The lowest value of lattice parameters calculated on the basis of Scherrer equation (5.17 Å in comparison with 5.27 Å for Ce_2Zr_2) was achieved for catalyst enriched in Zr. This discrepancy could be explained by the shrinkage of the lattice due to the Ce^{4+} (97 pm) replacement by smaller Zr^{4+} cations. In the case of Ce-rich $Ce_{2.96}Zr_{0.53}Ni$ catalyst the lattice parameter is higher (5.36 Å versus 5.27 Å for the support) which is ascribed to the expansion of the unit-cell due to the larger ionic radii of Ce^{4+} compared to Zr^{4+}.

In the case of the bimetallic Ni-Me catalysts (Fig. 2) besides diffraction patterns characteristic of fluorite structure and NiO species no evidence of Fe, Co or Rh oxides was observed. In the case of $Ce_2Zr_{1.51}NiRh$ catalyst it could be anticipated to low Rh loading (~0.5 wt.%) thus for $Ce_2Zr_{1.51}NiFe$ and $Ce_2Zr_{1.51}NiCo$ to different ionic radii than that of Ni (Fe^{2+} 61 pm, Co^{2+} 75 pm) and lower

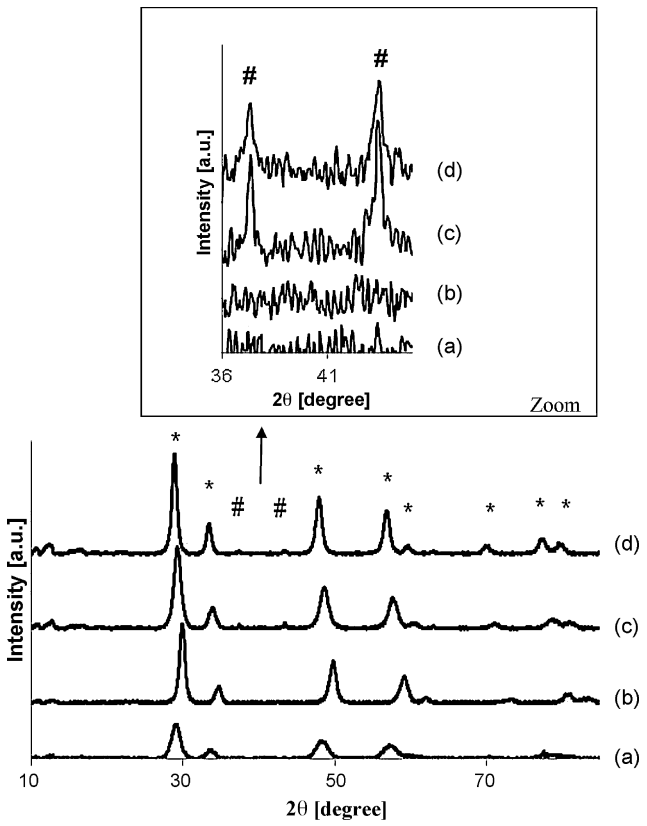

Fig. 1. XRD of freshly prepared catalyst (a) Ce_2Zr_2 (support); (b) $Ce_{0.6}Zr_{2.97}Ni_{0.43}$; (c) $Ce_2Zr_{1.51}Ni_{0.49}$; (d) $Ce_{2.96}Zr_{0.53}Ni_{0.51}$. (*)—face-centered cubic, fluorite structure, (#)—NiO species Zoom of the diffraction patterns of NiO

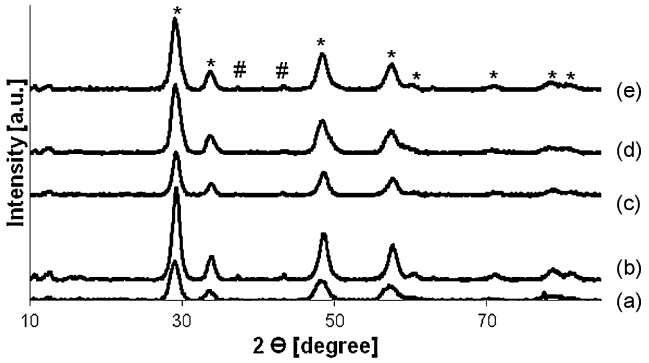

Fig. 2. XRD of freshly prepared catalyst (a) Ce_2Zr_2 (support); (b) $Ce_2Zr_{1.51}Ni_{0.49}$; (c) $Ce_2Zr_{1.51}Ni_{0.49}Co_{0.29}$; (d) $Ce_2Zr_{1.51}Ni_{0.49}Fe_{0.20}$; (e) $Ce_2Zr_{1.51}Ni_{0.49}Rh_{0.03}$. (*)—face-centered cubic, fluorite structure, (#)—NiO species.

loading (2 wt.% instead of 3 wt.%) what can facilitate the insertion of these cations into the Ce-Zr structure. Furthermore, the high dispersion of the metals could be also taken into account. The difference in loading is very low but it can be observed that the insertion of more then 3 wt.% of Ni results in rejection from the structure. The lattice parameters of $Ce_2Zr_{1.51}NiCo$, $Ce_2Zr_{1.51}NiFe$ and $Ce_2Zr_{1.51}NiRh$ catalysts are close to the one for $Ce_2Zr_{1.51}Ni$ thus the substitution of Ni by these cations does not result in the modification of the unit-cell.

The support particle sizes for all the catalysts and for the support are in the range of 5–9 nm, irrespective of Ce to Zr ratio and metals incorporation.

TPR profiles of support and Ni catalysts with different Ce and Zr content are shown in Fig. 3(a–d). TPR outline of Ce-Zr mixed oxide shows two characteristic peaks, one at 600 °C and second one at 780 °C (Fig. 3a). Since ZrO_2 did not show any reduction peak at this temperature range [13] it was assumed that all the consumed hydrogen comes from CeO_2 reduction. Low temperature peak could be ascribed to the reduction of surface CeO_2 while the high temperature one to the reduction of bulk CeO_2. The incorporation of Ni into Ce-Zr structure results in shifting these temperatures to lower values. The peaks at 380 °C and 420 °C could correspond to nickel (incorporated into the Ce-Zr structure) and ceria reduction (Fig. 3(b–d)). For the catalysts enriched in Ce a peak (Fig. 3(d)) and a shoulder (Fig. 3(c)) at 310 °C are observed. This can be assigned to the hydrogen consumption during the reduction of Ni rejected from the structure, that is in agreement with what was observed on the XRD diffractograms. This result confirms that the increase in Ce content leads to incomplete integration of Ni into the mixed oxide structure due to the lack of this peak for the other catalyst (Fig. 3(b)).

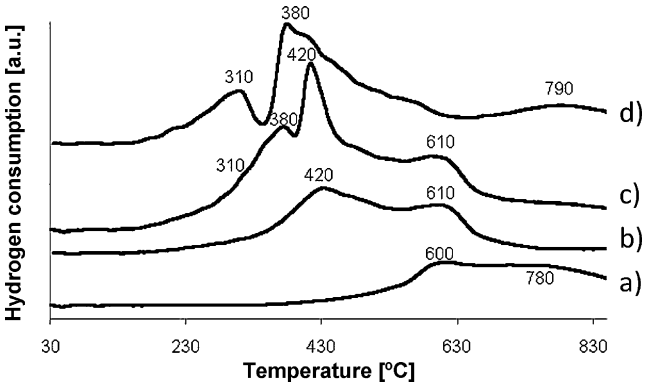

Fig. 3. TPR profiles of (a) Ce_2Zr_2 (support) and fresh catalysts with different Ce to Zr proportion (b) $Ce_{0.6}Zr_{2.97}Ni_{0.43}$; (c) $Ce_2Zr_{1.51}Ni_{0.49}$; (d) $Ce_{2.96}Zr_{0.53}Ni_{0.51}$.

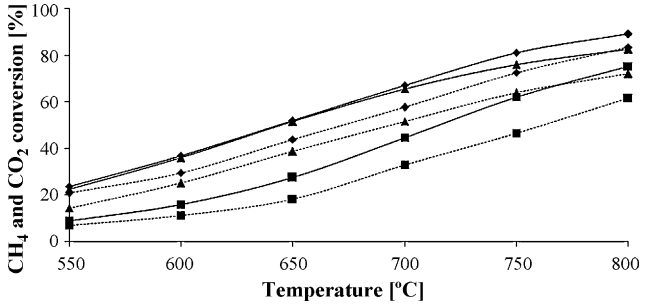

Fig. 4. CO_2 (–) and CH_4 (···) conversions over different catalysts (◆) $Ce_2Zr_{1.51}Ni_{0.49}$; (▲) $Ce_{0.6}Zr_{2.97}Ni_{0.43}$; (■) $Ce_{2.96}Zr_{0.53}Ni_{0.51}$. Reaction conditions: CH_4/CO_2/Ar 10/10/80; total space velocity equal to 30 L h^{-1} g^{-1}; catalysts were prior reduced in 5% H_2-95% Ar at 750 °C for 4 h.

3.2. Catalytic activity measurements

To find out the optimum Ce to Zr proportion, catalysts with varying Ce and Zr contents and constant nickel loading equal to 5 wt.% were tested in CO_2 reforming of methane reaction. Fig. 4 demonstrates the temperature dependence on catalytic activity for Ni-based catalysts. CH_4 conversion is lower than CO_2 one due to the presence of reverse water gas-shift reaction (RWGS) occurring simultaneously with CO_2 reforming of CH_4 [14]. The highest activity in both CO_2 and CH_4 conversion was observed over catalyst with nearly stoichiometric Ce to Zr ratio ($Ce_2Zr_{1.51}Ni$). The increase in Ce content leads to the drop in the activity, much significant than that for catalyst enriched in Zr. Whereas, the catalyst with the highest Zr content deactivates faster than what can be observed tracking the curve of CO_2 conversion at 750 °C during the long-term experiment (Fig. 5). The $Ce_2Zr_{1.51}Ni$ catalyst showing the highest activity in CO_2 reforming reaction is simultaneously the most stable one after 25 h time on stream with only 20% of deactivation. This catalyst was then chosen as a base to prepare bimetallic systems.

In Fig. 6 the variation in CO_2 conversion versus temperature for the bimetallic catalysts compared with monometallic Ni and support are presented. The CH_4 conversion results are not shown here due to the similar tendency of the curve as CO_2 conversion. The $Ce_2Zr_{1.51}NiRh$ catalyst exhibits the highest activity. On the contrary, for the other two catalysts where part of Ni was substituted by Co and Fe, the activity was nearly the same (in the case of $Ce_2Zr_{1.51}NiCo$) and lower (in the case of $Ce_2Zr_{1.51}NiFe$). To confirm the high activity of the $Ce_2Zr_{1.51}NiRh$ catalyst, the stability test was performed and the results are shown in Fig. 7. This catalyst demonstrated the best thermal stability with CO_2 conversion around 90% in the first hours of the reaction. The loss of activity ca. 11% was only observed after 50 h

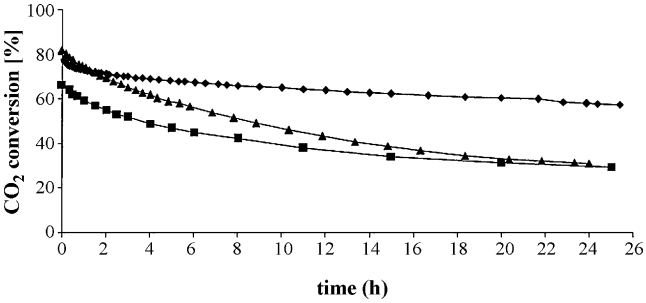

Fig. 5. Catalytic activity of CO_2 versus time on dry reforming of CH_4 for (◆) $Ce_2Zr_{1.51}Ni_{0.49}$; (▲) $Ce_{0.6}Zr_{2.97}Ni_{0.43}$; (■) $Ce_{2.96}Zr_{0.53}Ni_{0.51}$ at 750 °C. Reaction conditions: CH_4/CO_2/Ar 10/10/80; total space velocity equal to 30 L h^{-1} g^{-1}; catalysts were prior reduced in 5% H_2-95% Ar at 750 °C for 4 h.

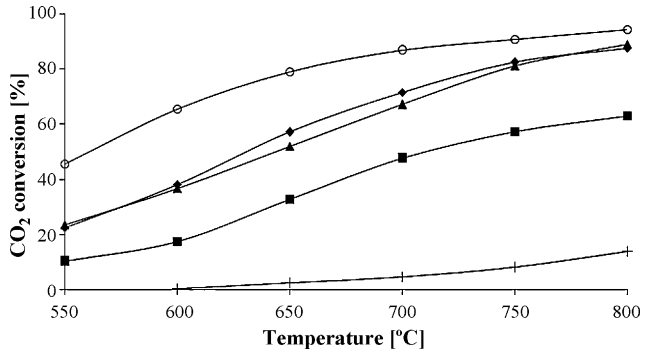

Fig. 6. Variation of CO_2 conversion with temperature over (+) Ce_2Zr_2 (support); (■) $Ce_2Zr_{1.51}Ni_{0.49}Fe_{0.20}$; (▲) $Ce_2Zr_{1.51}Ni_{0.49}$; (◆) $Ce_2Zr_{1.51}Ni_{0.49}Co_{0.29}$ and (○) $Ce_2Zr_{1.51}Ni_{0.49}Rh_{0.03}$. Reaction conditions: CH_4/CO_2/Ar 10/10/80; total space velocity equal to 30 L h^{-1} g^{-1}; catalysts were prior reduced in 5% H_2-95% Ar at 750 °C for 4 h.

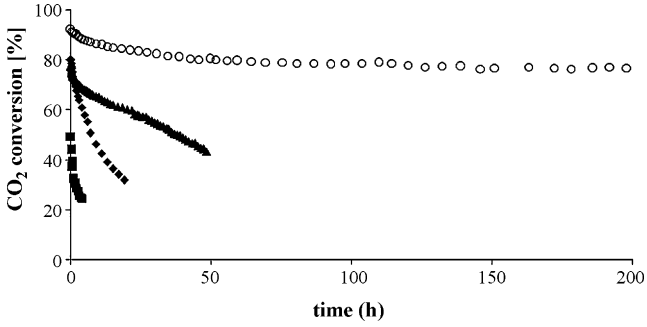

Fig. 7. CO_2 conversion as a function of time in dry reforming of methane at 750 °C over (○) $Ce_2Zr_{1.51}Ni_{0.49}Rh_{0.03}$; (◆) $Ce_2Zr_{1.51}Ni_{0.49}Co_{0.29}$; (■) $Ce_2Zr_{1.51}Ni_{0.49}Fe_{0.20}$; (▲) $Ce_2Zr_{1.51}Ni_{0.49}$. Reaction conditions: CH_4/CO_2/Ar 10/10/80; total space velocity equal to 30 L h^{-1} g^{-1}; catalysts were prior reduced in 5% H_2-95% Ar at 750 °C for 4 h.

of the test, however, it remains still constant for over 150 h with the CO_2 conversion ca. 80%. Whereas, for the other bimetallic catalysts the deactivation process starts very quickly reaching a drop of activity ca. 57% after 17 h for $Ce_2Zr_{1.51}$NiCo and 41% just after 2 h for $Ce_2Zr_{1.51}$NiFe.

The deactivation of the Ni-based catalysts could be realized due to the formation of carbonaceous deposits [15–17], different types of carbon [18,19] and metal sintering [20].

The results of thermogravimetric experiments under the reaction conditions for $Ce_2Zr_{1.51}$Ni and $Ce_2Zr_{1.51}$NiRh catalysts (not shown here) display that over the latter one the amount of carbon is greater than that for $Ce_2Zr_{1.51}$Ni. As it was previously shown the $Ce_2Zr_{1.51}$NiRh is very resistant in ageing process thus it is not the amount of carbon which decreases the activity, but the type of carbonaceous species. There are at least three types of carbon: carbides, graphite and carbon nanotubes. At the TEM images (not shown here) it can be seen that the addition of Rh prevents formation of carbon nanotubes in comparison to monometallic Ni catalyst. This allows us to suggest that these carbon nanotubes could be the poisons of catalysts in CO_2 reforming of CH_4.

4. Conclusions

The monometallic Ce-Zr-Ni and bimetallic Ce-Zr-Ni-Me catalysts were prepared by pseudo sol–gel method. The XRD diffractograms match well to face-centered cubic fluorite and showed small amount of nickel rejected from the host Ce-Zr structure which depends on Ce content. No diffraction patterns corresponding to iron, cobalt or rhodium oxides were observed.

It was demonstrated that $Ce_2Zr_{1.51}$Ni catalyst revealed the highest activity in CO_2 reforming of methane and a good stability during 25 h time on stream. The partial substitution of Ni by Rh (0.5 wt.%) resulted in improving both the activity and significantly the stability of the catalyst. It was observed that the deactivation process is not associated with the presence of carbon but with the type of carbon on the catalyst surface.

Acknowledgment

The authors wish to acknowledge the financial support from European Union under Project *Era Chemistry*.

References

[1] J. Ascencion Montoya, E. Romero, A. Monzon, C. Guimon, Stud. Surf. Sci. Catal. 130 (2000) 3669.
[2] S. Xu, X. Wang, Fuel 84 (2005) 563.
[3] Y. Mukainakano, B. Li, S. Kado, T. Miyazawa, K. Okumura, T. Miyao, S. Naito, K. Kunimori, K. Tomishige, Appl. Catal. A 318 (2007) 252.
[4] F. Pompeo, N. Nichio, M. Souza, D. Cesar, O. Ferretti, M. Schmal, Appl. Catal. A 316 (2007) 175.
[5] A. Ballarini, S. De Miguel, E.L. Jablonski, O. Scelza, A. Castro, Catal. Today 107–108 (2005) 481.
[6] J.C. Vargas, S. Libs, A.C. Roger, A. Kiennemann, Catal. Today 107–108 (2005) 417.
[7] J.C. Vargas, A.C. Roger, A. Kiennemann, Chem. Eng. Trans. 4 (2004) 247.
[8] M. Virginie, M. Araque, A.C. Roger, J.C. Vargas, A. Kiennemann, Catal. Today 138 (2008) 21.
[9] H.C. Yao, Y.F. Yu Yao, J. Catal. 86 (1984) 265.
[10] H.S. Roh, H.S. Potdar, K.W. Jun, J.W. Kim, Y.S. Oh, Appl. Catal. A 276 (2004) 231.
[11] J.C. Vargas, E. Vanhaecke, A.C. Roger, A. Kiennemann, Stud. Surf. Sci. Catal. 147 (2004) 115.
[12] F. Romero-Sarria, J.C. Vargas, A.C. Roger, A. Kiennemann, Catal. Today 133 (2008) 149.
[13] W.H. Dong, H.S. Roh, K.W. Jun, S.E. Park, Y.S. Oh, Appl. Catal. A 226 (2002) 63.
[14] M.C.J. Bradford, M.A. Vannice, Catal. Rev. Sci. Eng. 41 (1999) 1.
[15] S. Wang, G.Q. Lu, Ind. Eng. Chem. Res. 38 (1999) 2615.
[16] Y.H. Chen, J. Ren, Catal. Lett. 29 (1994) 39.
[17] Z.L. Zhang, X.E. Verykios, Catal. Today 21 (1994) 589.
[18] Y.H. Chin, D.L. King, H.S. Roh, Y. Wang, S.M. Heald, J. Catal. 244 (2006) 153.
[19] J. Zhang, H. Wang, A.K. Dalai, J. Catal. 249 (2007) 300.
[20] V.C.H. Kroll, H.M. Swaan, C. Mirodatos, J. Catal. 161 (1996) 409.